

# Simple Design of a Tunable Quadruple-Broadband Terahertz Metamaterial Absorber Based on VO<sub>2</sub>

Kwang-Jin Ri<sup>1,\*</sup>, Dae-Song Pak<sup>2</sup>, Chung-Ho Ri<sup>1</sup>

<sup>1</sup>Department of Physics, University of Sciences, Pyongyang, Democratic People's Republic of Korea

<sup>2</sup>Department of Physics, Kim Hyong Jik University of Education, Pyongyang, Democratic People's Republic of Korea

## Email address:

rkj1994@star-co.net.kp (Kwang Jin Ri)

\*Corresponding author

## To cite this article:

Kwang-Jin Ri, Dae-Song Pak, Chung-Ho Ri. Simple Design of a Tunable Quadruple-Broadband Terahertz Metamaterial Absorber Based on VO<sub>2</sub>. *Advances in Materials*. Vol. 12, No. 4, 2023, pp. 45-52. doi: 10.11648/j.am.20231204.11

**Received:** October 18, 2023; **Accepted:** November 9, 2023; **Published:** November 21, 2023

---

**Abstract:** Tunable multi-broadband terahertz (THz) metamaterial absorbers (MAs) can effectively act as THz amplitude modulators, which are the essential components for the future THz communication systems. Till now, various tunable multi-broadband THz MAs including tunable dual-broadband and triple-broadband absorbers have been investigated. However, there are few researches on tunable quadruple-broadband THz MAs. In this work, a simple design of tunable quadruple-broadband THz MA based on VO<sub>2</sub> is proposed. The proposed absorber possesses four broad absorption bands with absorptivity over 90% in frequency ranges of 0.54-2.30 THz, 3.67-5.33 THz, 6.72-8.4 THz and 9.72-11.47 THz, and the corresponding absorption bandwidths reach 1.76 THz, 1.66 THz, 1.68 THz and 1.75 THz, respectively. Moreover, we can dynamically control the absorptivity of four absorption bands by varying VO<sub>2</sub> conductivity. Thus, the proposed absorber possesses the modulation depths of 79.15%, 49.71%, 33.03% and 21.98% at 1.48 THz, 4.46 THz, 7.45 THz and 10.44 THz, respectively. The physical origin of quadruple-broadband perfect absorption is revealed with aid of electric field distributions at resonant frequencies. We also investigate the effects of incidence angle and polarization angle on the quadruple-broadband perfect absorption. The proposed absorber has broad application prospects in THz imaging, modulating, detecting and sensing owing to its excellent absorption characteristics.

**Keywords:** Terahertz, Metamaterial, Quadruple, Tunable, Vanadium Dioxide, Bandwidth

---

## 1. Introduction

Today, THz technology has been widely introduced in 5G, 6G communication [1], security [2], biomedicine [3] and nondestructive detection [4]. Particularly, THz MAs have drawn more and more attention because of their critical roles in many THz functional devices. In 2008, Tao and his colleagues [5] firstly proposed the narrowband THz MA. Thereafter, a great number of THz MAs have been developed to obtain multi-band and broadband perfect absorptions [6-16]. However, these MAs are designed and fabricated mainly by using the metal-dielectric-metal structure. Such a configuration unavoidably results in the difficulty in controlling the absorption performances. In fact, the preferred MAs for practical application fields are tunable THz MAs.

Over the past years, tunable THz MAs based on active

materials [17-27] have achieved tremendous progress. Particularly, many researchers have investigated VO<sub>2</sub>-based tunable broadband THz MAs [28-35]. Meanwhile, recently, many efforts have been focused on the design of tunable multi-broadband THz MAs. In future, THz communication systems will require the tunable multi-broadband THz MAs to promote multi-task systems [36]. Moreover, these absorbers are also very useful for sensing applications [37]. In 2020, a tunable dual-broadband THz MA using VO<sub>2</sub> material was designed and investigated by Jiao et al. [38]. This absorber has two broad absorption bands with absorptivity over 90% in frequency ranges of 1.87 THz-4.19 THz and 8.70 THz-10.73 THz, and its absorptivity can be dynamically changed between 2% and 94%. Huang et al. [39] designed an active controllable dual-broadband THz MA with VO<sub>2</sub> resonator, the absorption bandwidths of 80% absorptivity are 0.88 THz and 0.77 THz. Moreover, its

absorptivity can be adjusted from 20% to 90%. In 2022, Feng *et al.* [40] designed a tunable dual-broadband THz MA based on VO<sub>2</sub> material. The absorption bandwidths of 90% absorptivity are 3.4 THz and 3.06 THz, and its absorptivity can be changed from 2% to 100%. In 2023, Ri *et al.* [41] designed a tunable dual-broadband THz MA with slotted VO<sub>2</sub> resonator, the absorption bandwidths of 90% absorptivity can reach 3.41 THz and 3.25 THz. In addition, its absorptivity can be changed from 20% to over 90%. In the latest work [42], a novel tunable triple-broadband THz MA with single VO<sub>2</sub> ring was proposed, the absorption bandwidths of 90% absorptivity were 2.35 THz, 2.30 THz and 2.40 THz, and the absorptivity can be dynamically changed from 20% to over 90%. However, recent researches on tunable multi-broadband MAs are mainly limited to the tunable dual-broadband and triple-broadband THz MAs, no further research on tunable quadruple-broadband THz MA

has been carried out.

In this work, we propose a novel tunable quadruple-broadband THz MA with single VO<sub>2</sub> resonator, whose absorptivity exceeds 90% in the four frequency ranges of 0.54-2.30 THz, 3.67-5.33 THz, 6.72-8.4 THz and 9.72-11.47 THz, and the corresponding absorption bandwidths are 1.76 THz, 1.66 THz, 1.68 THz and 1.75 THz, respectively. Compared with previous tunable multi-broadband THz absorbers, our designed absorber has the excellent characteristics of quadruple-band, broadband, and simple resonant structure. Moreover, the absorptivity of four absorption bands can be continuously adjusted under thermal control. The physical origin of quadruple-broadband absorption is clarified by studying the electric field distributions at resonant frequencies. Finally, we investigate the effects of incidence and polarization angles on quadruple-broadband perfect absorption.

## 2. Design and Simulation

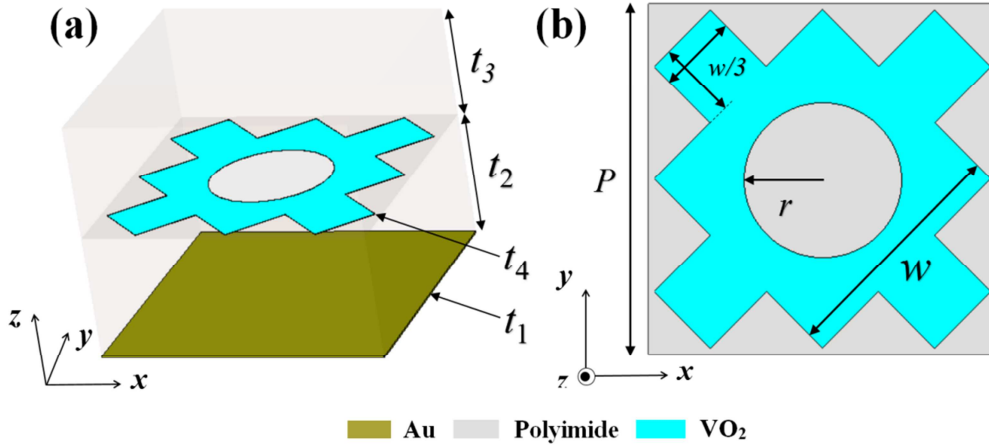


Figure 1. Schematic diagram of the proposed absorber: (a) 3D structure of the unit cell, (b) front view of the unit cell.

The unit cell of proposed absorber possesses the gold-polyimide-VO<sub>2</sub>-polyimide configuration as shown in Figure 1. Such a configuration has already been validated as the efficient absorber structure in the previous studies [41, 42]. The gold ground plane has the thickness of  $t_1 = 0.4 \mu\text{m}$  and the conductivity of  $\sigma = 4.561 \times 10^7 \text{ S/m}$ . The polyimide material has the dielectric constant of  $\epsilon = 3(1 + i0.06)$  [43]. The thickness of VO<sub>2</sub> resonator is  $t_4 = 0.1 \mu\text{m}$  and its optical dielectric constant is represented by the Drude model [44]:

$$\epsilon(\omega) = \epsilon_\infty - \frac{\omega_p^2(\sigma)}{(\omega^2 + i\gamma\omega)} \quad (1)$$

where,  $\epsilon_\infty = 12$  and  $\gamma = 5.75 \times 10^{13} \text{ rad/s}$  stand for the high-frequency permittivity and the collision frequency, respectively. The plasma frequency is given as:

$$\omega_p^2(\sigma) = \frac{\sigma_{\text{VO}_2}}{\sigma_0} \omega_p^2(\sigma_0) \quad (2)$$

with  $\sigma_0 = 3 \times 10^5 \text{ S/m}$  and  $\omega_p(\sigma_0) = 1.4 \times 10^{15} \text{ rad/s}$ . The conductivities of VO<sub>2</sub> ( $\sigma_{\text{VO}_2}$ ) are  $2 \times 10^5 \text{ S/m}$  and  $200 \text{ S/m}$  at  $T = 350 \text{ K}$  and  $T = 300 \text{ K}$ , respectively [45].

We extracted the geometrical parameters of the unit cell through the optimization process with the frequency-domain solver in a CST Microwave Studio software. In our simulations, unit cell boundary conditions are applied in x- and y- directions and open boundary condition is applied in z-direction. Moreover, the proposed absorber is exposed to normally incident transverse electric (TE) and transverse magnetic (TM) waves. The absorptivity of the proposed absorber can be expressed as  $A(\omega) = 1 - |S_{11}(\omega)|^2 - |S_{21}(\omega)|^2$ , where  $|S_{11}(\omega)|^2$  and  $|S_{21}(\omega)|^2$  stand for reflection and transmission, respectively. For the case of proposed absorber, transmission  $|S_{21}(\omega)|^2$  is close to zero on account of the gold ground plane. Then, the absorptivity can be calculated as  $A(\omega) = 1 - |S_{11}(\omega)|^2$ .

The main objective of optimization process is to simultaneously obtain quadruple-band absorption and broadband absorption at  $T = 350 \text{ K}$ . We first simulated the

absorption performance of proposed absorber for different values of  $t_2$  while other geometrical parameters remain unchanged. Figure 2(a) shows that the proposed absorber possesses four wide absorption bands with absorptivity over 90% for  $t_2 = 30 \mu\text{m}$ . After the thickness of polyimide substrate  $t_2$  is selected, other geometrical parameters should be optimized by turns to further improve the

quadruple-broadband absorption. Figure 2(b)-2(e) display the absorption curves of proposed absorber for different values of the thickness of polyimide substrate ( $t_3$ ), periodic length of unit cell ( $P$ ), side length of  $\text{VO}_2$  resonator ( $w$ ), radius of circular hole ( $r$ ), respectively. Consequently, the optimized values of geometrical parameters are  $t_2 = 30 \mu\text{m}$ ,  $t_3 = 28 \mu\text{m}$ ,  $P = 70 \mu\text{m}$ ,  $w = 47 \mu\text{m}$ ,  $r = 15 \mu\text{m}$ .

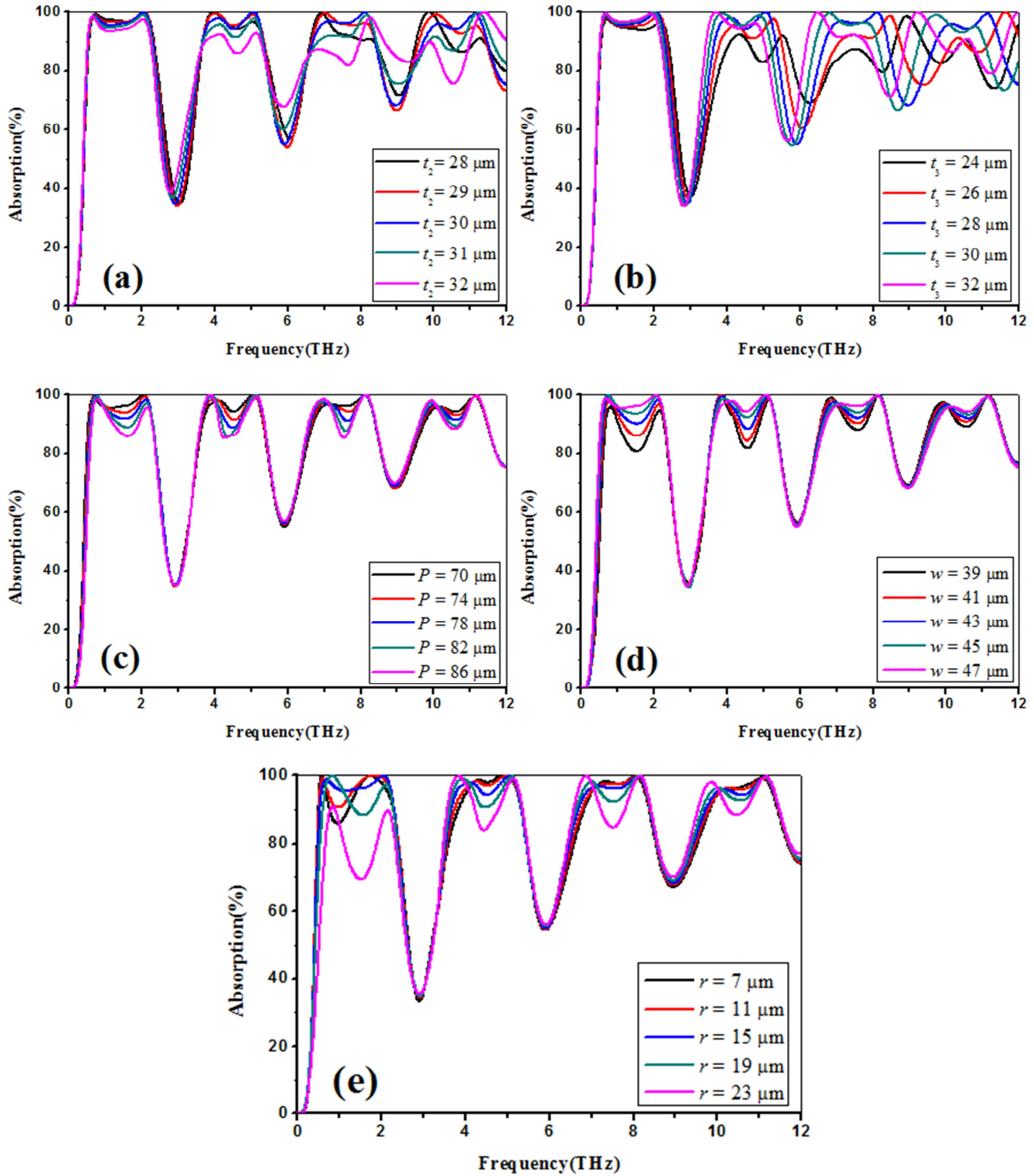


**Figure 2.** Absorption curves of the proposed absorber with different geometrical parameters: (a)  $t_2$ , (b)  $t_3$ , (c)  $P$ , (d)  $w$  and (e)  $r$ .

### 3. Results and Discussion

The absorption and reflection curves of the tunable quadruple-broadband THz MA with optimized geometrical parameters are plotted in Figure 3. It can be found that the proposed absorber has eight absorption peaks at 0.68 THz, 2.05 THz, 4.10 THz, 5.06 THz, 7.11 THz, 8.11 THz, 10.14 THz and 11.12 THz with absorptivities of 98.88%, 99.86%, 97.88%, 99.96%, 97.01%, 99.81, 96.01% and 99.39%, respectively. These eight absorption peaks couple together to form four broad absorption bands. The absorptivity of tunable quadruple-broadband THz MA is over 90% in four frequency ranges of 0.54-2.30 THz, 3.67-5.33 THz, 6.72-8.4 THz and 9.72-11.47 THz, and its absorption bandwidths are 1.76 THz, 1.66 THz, 1.68 THz and 1.75 THz, respectively.

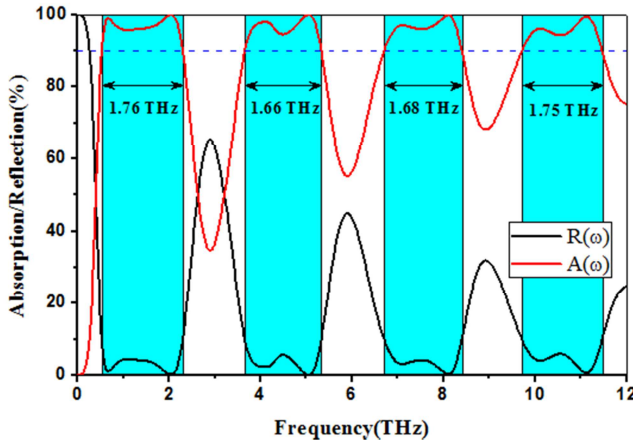


**Figure 3.** Absorption and reflection curves of the proposed absorber under TE wave at  $T=350$  K.

The absorption tunability of proposed absorber is also investigated. The conductivity of VO<sub>2</sub> changes with environmental temperature. Then, since the permittivity of VO<sub>2</sub> is influenced by its conductivity, we are able to tune the absorptivity of proposed absorber under thermal control. As shown in Figure 4, with the increase of conductivity of VO<sub>2</sub>, the absorptivities of four absorption bands continuously increase from 20% to 96.1%, from 47.4% to 94.3%, from 64.2% to 96% and from 73.8% to 94.6%, respectively. The modulation depth, defined as  $MD = (A_m - A_i)/A_m \times 100$  is a critical factor of the tunable MA, where  $A_m$  and  $A_i$  stand for the absorptivities for

metallic and insulator states of VO<sub>2</sub>, respectively [46]. This absorber possesses the modulation depths of 79.15%, 49.71%, 33.03% and 21.98% at 1.48 THz, 4.46 THz, 7.45 THz and 10.44 THz, respectively.

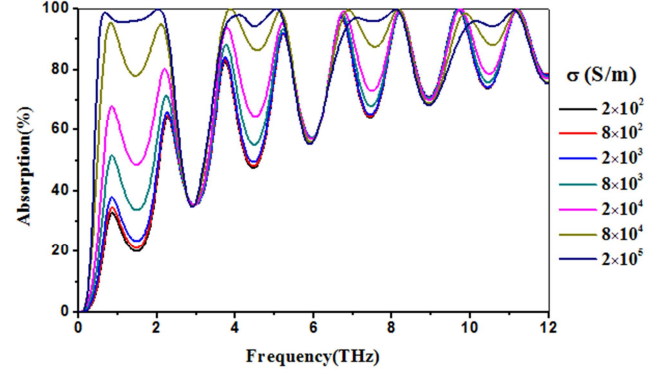


**Figure 4.** Absorption curves of the proposed absorber with different conductivities of VO<sub>2</sub>.

Here, we compared the absorption performances of tunable quadruple-broadband THz MA with other results reported in similar studies (see Table 1). Despite the simple absorber structure as shown in Figure 1, our absorber has good tunable quadruple-broadband absorption performance. It is natural that when the number of absorption bands increases in the limited simulation frequency range of 0-12 THz, the bandwidth of each absorption band becomes narrower. So, our absorber has broad application prospects in THz modulators, sensors, switches and detectors.

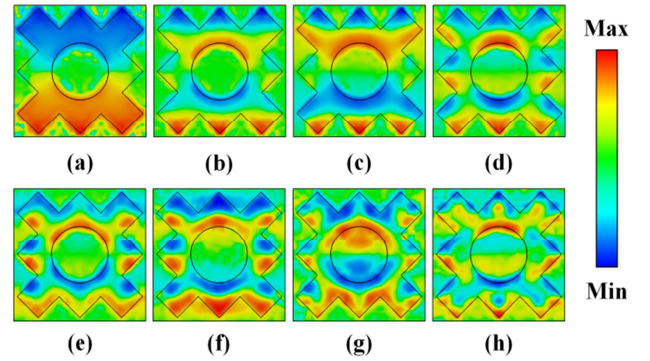


**Figure 5.** Electric field ( $E_z$ ) distributions at resonant frequencies: (a)  $f_1=0.68$  THz, (b)  $f_2=2.05$  THz, (c)  $f_3=4.10$  THz, (d)  $f_4=5.06$  THz, (e)  $f_5=7.11$  THz, (f)  $f_6=8.11$  THz, (g)  $f_7=10.14$  THz, (h)  $f_8=11.12$  THz.

**Table 1.** Comparison of the proposed absorber with other studies.

Ref.	Absorption Bandwidth (THz)	Adjustable Material	Tunable Range (%)	Thickness ( $\mu\text{m}$ )
[38]	2.32, 2.03	VO <sub>2</sub>	2-94	12.28
[39]	0.88, 0.77	VO <sub>2</sub>	20-90	35.3
[40]	3.40, 3.06	VO <sub>2</sub>	2-100	25.51
[41]	3.41, 3.25	VO <sub>2</sub>	20-90	27.8
[42]	2.35, 2.30, 2.40	VO <sub>2</sub>	20-90	44.4
This work	1.76, 1.66, 1.68, 1.75	VO <sub>2</sub>	20-96	58.5

To illustrate the physical origin of quadruple-broadband perfect absorption, we studied the electric field ( $E_z$ )

distributions at the eight resonant modes ( $f_1, f_2, f_3, f_4, f_5, f_6, f_7$  and  $f_8$ ). The simulated electric field ( $E_z$ ) distributions on the



x-y plane are plotted in Figure 5. As shown in Figure 5(a), at  $f_1=0.68$  THz, the strong electric field concentrates in lower and upper areas of VO<sub>2</sub> resonator, thus producing a dipole resonance. At  $f_2=2.05$  THz, the electric field is strongly localized in the outer and inner edges except for left and right sides of VO<sub>2</sub> resonator as shown in Figure 5(b). Such a distribution produces a quadrupole resonance. Thus, the first broad absorption band is attributed to the dipole and quadrupole resonances. As shown in Figure 5(c)-5(h), at  $f_3=4.10$  THz,  $f_4=5.06$  THz,  $f_5=7.11$  THz,  $f_6=8.11$  THz,  $f_7=10.14$  THz and  $f_8=11.12$  THz, the electric fields are strongly distributed on the inner and outer edges of VO<sub>2</sub> resonator, thus generating the high-order resonances. So, the second, third, and fourth broad absorption bands originate from the combination of similar high-order resonances.

Moreover, we further investigated the physical origin of quadruple-broadband absorption by means of LC circuit resonance and standing wave resonance. In accordance with refs. [47, 48], the resonant frequency of MA is calculated as:

$$f_j \approx (2j-1) \frac{c}{2nl}, j=1,2,3,\dots \quad (3)$$

where  $c$ ,  $l$ , and  $n$  stand for the light speed in vacuum, the

length of resonator, and the index of dielectric substrate, respectively. According to Eq. (3), the fundamental mode ( $j=1$ ) and its odd resonant modes are only valid. The absorption peaks of MA originate from these resonance modes. For example, the resonant frequency for the case of  $j=2$  must be 3 times greater than the resonant frequency of  $j=1$ . Table 2 shows the resonant frequencies of the proposed absorber with different VO<sub>2</sub> conductivities (see Figure 4). Here,  $f_{\text{average}}$  are the average values of resonant frequencies for the cases of  $f_1$ - $f_8$ , and  $f_{\text{theoretical}}$  are the theoretical frequencies calculated by Eq. (3). It can be seen from Table 2 that the average of second resonant frequencies ( $f_{2,\text{av}}=2.20$  THz) is approximately 3 times of the average of first resonant frequencies ( $f_{1,\text{av}}=0.82$  THz). Similarly,  $f_{3,\text{av}}=3.82$  THz,  $f_{4,\text{av}}=5.19$  THz,  $f_{5,\text{av}}=6.81$  THz,  $f_{6,\text{av}}=8.19$  THz,  $f_{7,\text{av}}=9.79$  THz and  $f_{8,\text{av}}=11.20$  THz are roughly five, seven, nine, eleven, thirteen and fifteen times of  $f_{1,\text{av}}=0.82$  THz, respectively. We can also know that there are some errors between  $f_{\text{average}}$  and  $f_{\text{theoretical}}$ . The reason is that Eq. (3) neglects the dielectric dispersion of polyimide layer. Consequently, we can conclude that the quadruple-broadband perfect absorption is attributed to the fundamental and high-order resonances of VO<sub>2</sub> resonator.

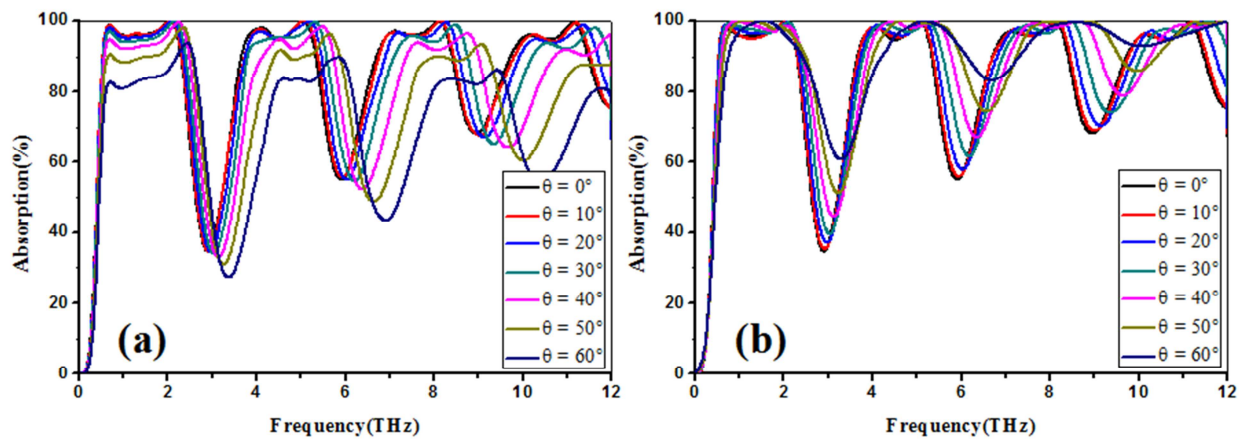


Figure 6. Absorption curves of the proposed absorber for different values of incidence angle at (a) TE and (b) TM waves.

Table 2. Resonant frequencies of the proposed absorber with different values of VO<sub>2</sub> conductivity.

Conductivity of VO <sub>2</sub> (S/m)	Resonant frequency (THz)							
	$f_1$	$f_2$	$f_3$	$f_4$	$f_5$	$f_6$	$f_7$	$f_8$
200	0.86	2.28	3.75	5.24	6.72	8.22	9.70	11.22
800	0.86	2.28	3.75	5.23	6.72	8.22	9.70	11.22
2000	0.86	2.26	3.75	5.23	6.72	8.22	9.70	11.22
8000	0.86	2.24	3.76	5.23	6.74	8.22	9.72	11.20
20000	0.85	2.21	3.79	5.20	6.76	8.20	9.75	11.20
80000	0.82	2.11	3.89	5.14	6.90	8.17	9.87	11.18
200000	0.68	2.05	4.10	5.06	7.11	8.11	10.14	11.12
$f_{\text{average}}$	0.82	2.20	3.82	5.19	6.81	8.19	9.79	11.20
$f_{\text{theoretical}}$	-	2.46	4.10	5.74	7.38	9.02	10.66	12.30

In order to examine the incidence angle dependence of tunable quadruple-broadband THz MA, we analyzed the absorption curves of proposed absorber with different incidence angles under TE and TM waves. As shown in Figure 6(a), the increase of incidence angle under TE wave results in

the blue-shift of four absorption bands, but the absorptivity of each absorption band still remains over 80% for large incidence angle of 50°. Under TM wave, the increase of incidence angle also results in the blue-shift of four absorption bands as shown in Figure 6(b), but the absorptivity of each

absorption band still exceeds 90% for large incidence angles up to 60°. Thus, our absorber possesses good incidence angle

stability.

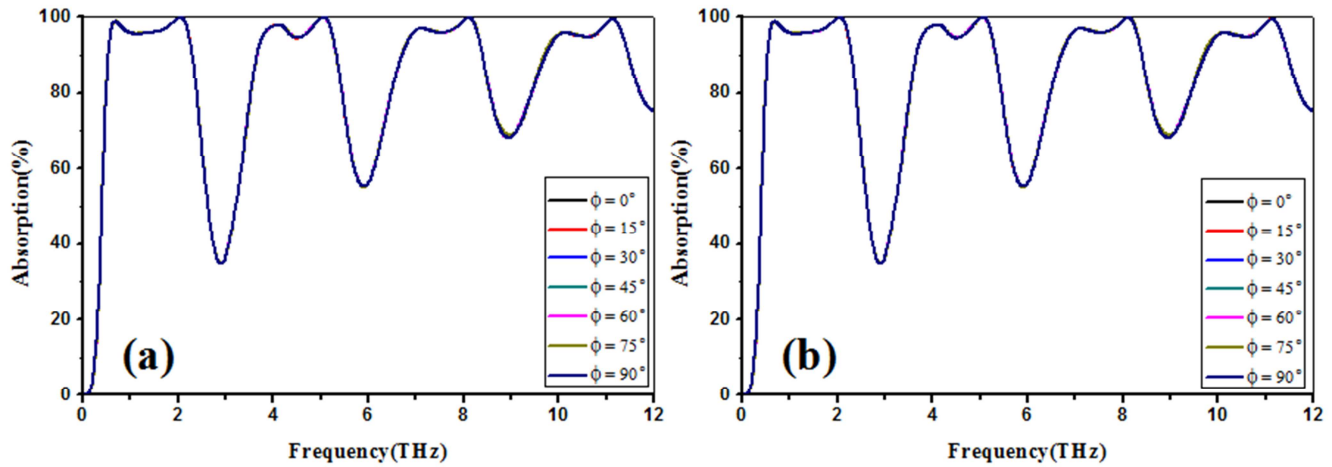


**Figure 7.** Absorption curves of the proposed absorber for different values of polarization angle at (a) TE and (b) TM waves.

Finally, we simulated the absorption performance of proposed absorber for different values of polarization angle at TE and TM waves. Our designed absorber possesses good polarization-insensitivity owing to the fourfold rotational symmetry as shown in Figure 7.

## 4. Conclusion

Until now, various designs on tunable dual-broadband/triple-broadband THz MAs have been proposed. However, no further research on the tunable quadruple-broadband THz MA has been done. In this work, we have proposed a simple design of tunable quadruple-broadband THz MA based on VO<sub>2</sub>. Simulation results show that the proposed absorber has four broad absorption bands with absorptivity above 90% in frequency ranges of 0.54-2.30 THz, 3.67-5.33 THz, 6.72-8.4 THz and 9.72-11.47 THz, and the corresponding absorption bandwidths reach 1.76 THz, 1.66 THz, 1.68 THz and 1.75 THz, respectively. The absorptivities of four absorption bands can be dynamically tuned from 20% to 96.1%, from 47.4% to 94.3%, from 64.2% to 96% and from 73.8% to 94.6%, respectively. The overlap of fundamental and high-order resonances on the single VO<sub>2</sub> resonator results in the quadruple-broadband perfect absorption. Furthermore, the proposed absorber possesses wide incidence angle stability and polarization-insensitivity. Thus, the proposed absorber has broad application prospects in THz imaging, modulating, detecting and sensing.

## Competing Interests

The authors declare no competing interests.

## Author Contributions

K. J. Ri conceived the idea, performed the simulations and

wrote the manuscript. D. S. Pak analyzed the results and assisted the revision of the manuscript. C. H. Ri supervised the entire project. All authors have read and approved the final manuscript.

## Data Availability

All data used to support the findings in this study are included within the paper.

## ORCID

Kwang-Jin Ri: <https://orcid.org/0009-0002-2603-2724>

## Acknowledgments

This work is supported by the Key Basic Research Project of DPR Korea.

## References

- [1] A. A. Musaed, S. S. Al-Bawri, M. T. Islam, A. J. A. Al-Gburi, M. J. Singh, Tunable Compact Metamaterial-Based Double-Negative/Near-Zero Index Resonator for 6G Terahertz Wireless Applications, *Materials* 15 (2022) 5608.
- [2] M. Tonouchi, Cutting-edge terahertz technology, *Nature Photonics* 1 (2007) 97–105.
- [3] H. Luo, Y. Cheng, Thermally tunable terahertz metasurface absorber based on all dielectric indium antimonide resonator structure, *Optical Materials* 102 (2020) 109801.
- [4] S. Fan, T. Li, J. Zhou, X. Liu, X. Liu, H. Qi, Z. Mu, Terahertz non-destructive imaging of cracks and cracking in structures of cement based materials. *AIP Advances* 7 (2017) 115202.
- [5] H. Tao, N. I. Landy, C. M. Bingham, X. Zhang, R. D. Averitt, W. J. Padilla, A metamaterial absorber for the terahertz regime: design, fabrication and characterization, *Opt. Express* 16 (2008) 7181-7188.

- [6] B. X. Wang, C. Tang, Q. S. Niu, Y. H. He, T. Chen, Design of Narrow Discrete Distances of Dual-/Triple-Band Terahertz Metamaterial Absorbers, *Nanoscale Research Letters* 14 (2019) 64.
- [7] T. Meng, D. Hu, Q. Zhu, Design of a five-band terahertz perfect metamaterial absorber using two resonators, *Optics Communications* 415 (2018) 151–155.
- [8] Y. Z. Wen, W. Ma, J. Bailey, G. Matmon, X. M. Yu, Broadband Terahertz Metamaterial Absorber Based on Asymmetric Resonators With Perfect Absorption, *IEEE TRANSACTIONS ON TERAHERTZ SCIENCE AND TECHNOLOGY* 5 (2015) 406–411.
- [9] B. X. Wang, Q. Xie, G. X. Dong, H. X. Zhu, Broadband terahertz metamaterial absorber based on coplanar multi-strip resonators, *Journal of Materials Science: Materials in Electronics* 28 (2017) 17215–17220.
- [10] Y. Z. Cheng, Y. Nie, R. Z. Gong, A polarization-insensitive and omnidirectional broadband terahertz metamaterial absorber based on coplanar multi-squares films, *Optics & Laser Technology* 48 (2013) 415–421.
- [11] Y. Y. Lu, J. N. Li, S. H. Zhang, J. H. Sun, J. Q. Yao, Polarization-insensitive broadband terahertz metamaterial absorber based on hybrid structures, *Applied Optics* 57 (2018) 6269–6275.
- [12] J. B. Sun, L. Y. Liu, G. Y. Dong, J. Zhou, An extremely broad band metamaterial absorber based on destructive interference, *Opt. Express* 19 (2011) 21155–21162.
- [13] B. X. Wang, L. L. Wang, G. Z. Wang, W. Q. Huang, X. F. Li, X. Zhai, A simple design of ultra-broadband and polarization insensitive terahertz metamaterial absorber, *Appl. Phys. A* 115 (2014) 1187–1192.
- [14] Y. Q. Ye, Y. Jin, S. L. He, Omnidirectional, polarization-insensitive and broadband thin absorber in the terahertz regime, *Journal of the Optical Society of America B* 27 (2010) 498–504.
- [15] X. J. He, S. T. Yan, Q. X. Ma, Q. F. Zhang, P. Jia, F. M. Wu, J. X. Jiang, Broadband and polarization-insensitive terahertz absorber based on multilayer metamaterials, *Optics Communications* 340 (2015) 44–49.
- [16] B. X. Wang, L. L. Wang, G. Z. Wang, W. Q. Huang, X. F. Li, X. Zhai, Theoretical Investigation of Broadband and Wide-Angle Terahertz Metamaterial Absorber, *IEEE Photon. Technol. Lett.* 26 (2014) 111–114.
- [17] F. Chen, Y. Z. Cheng, H. Luo, A Broadband Tunable Terahertz Metamaterial Absorber Based on Single-Layer Complementary Gammadion-Shaped Graphene, *Materials* 13 (2020) 860.
- [18] J. Zhu, C. S. Wu, Y. H. Ren, Broadband terahertz metamaterial absorber based on graphene resonators with perfect absorption, *Results in Physics* 26 (2021) 104466.
- [19] L. Liu, W. W. Liu, Z. Y. Song, Ultra-broadband terahertz absorber based on a multilayer graphene metamaterial, *J. Appl. Phys.* 128 (2020) 093104.
- [20] S. J. Guo, C. X. Hu, H. F. Zhang, Unidirectional ultrabroadband and wide-angle absorption in graphene-embedded photonic crystals with the cascading structure comprising the Octonacci sequence, *Journal of the Optical Society of America B*, 37 (2020) 2678–2687.
- [21] W. W. Liu, J. S. Xu, Z. Y. Song, Bifunctional terahertz modulator for beam steering and broadband absorption based on a hybrid structure of graphene and vanadium dioxide, *Optics Express* 29 (2021) 23331–23340.
- [22] W. W. Liu, Z. Y. Song, Terahertz absorption modulator with largely tunable bandwidth and intensity, *Carbon* 174 (2021) 617–624.
- [23] C. Q. Li, Z. Y. Song, Tailoring terahertz wavefront with state switching in VO<sub>2</sub> Pancharatnam-Berry metasurfaces, *Optics and Laser Technology* 157 (2023) 108764.
- [24] R. X. Nie, C. H. He, R. X. Zhang, Z. Y. Song, Vanadium dioxide-based terahertz metasurfaces for manipulating wavefronts with switchable polarization, *Optics and Laser Technology* 159 (2023) 109010.
- [25] K. V. Sreekanth, S. Han, R. Singh, Ge<sub>2</sub>Sb<sub>2</sub>Te<sub>5</sub>-based tunable perfect absorber cavity with phase singularity at visible frequencies, *Adv. Mater.* 30 (2018) 1706696.
- [26] Y. Qu et al. Dynamic thermal emission control based on ultrathin plasmonic metamaterials including phase-changing material GST, *Laser Photon. Rev.* 11 (2017) 1700091.
- [27] R. N. Dao, X. R. Kong, H. F. Zhang, X. R. Su, A tunable broadband terahertz metamaterial absorber based on the vanadium dioxide, *Optik-International Journal for Light and Electron Optics* 180 (2019) 619–625.
- [28] Y. C. Liu, Y. X. Qian, F. R. Hu, M. Z. Jiang, L. H. Zhang, A dynamically adjustable broadband terahertz absorber based on a vanadium dioxide hybrid metamaterial, *Results in Physics* 19 (2020) 103384.
- [29] N. L. Mou, B. Tang, J. Z. Li, H. X. Dong, L. Zhang, Switchable ultra-broadband terahertz wave absorption with VO<sub>2</sub>-based metasurface, *Sci. Rep.* 12 (2022) 2501.
- [30] P. Zhang, G. Chen, Z. Hou, Y. Zhang, J. Shen, C. Li, M. Zhao, Z. Gao, Z. Li, T. Tang, Ultra-broadband tunable terahertz metamaterial absorber based on double-layer vanadium dioxide square ring arrays, *Micromachines* 13 (2022) 669.
- [31] X. Wang, G. Wu, Y. Wang, J. Liu, Terahertz broadband adjustable absorber based on VO<sub>2</sub> multiple ring structure, *Applied Sciences* 13 (2023) 252.
- [32] J. J. Bai, S. S. Zhang, F. Fan, S. S. Wang, X. D. Sun, Y. P. Miao, and S. J. Chang, Tunable broadband THz absorber using vanadium dioxide metamaterials. *Optics Communications* 452 (2019) 292–295.
- [33] Z. Y. Song, K. Wang, J. W. Li, Q. H. Liu, Broadband tunable terahertz absorber based on vanadium dioxide metamaterials, *Optics Express* 26 (2018) 7148–7154.
- [34] C. Gandhi, P. R. Babu, K. Senthilnathan, Ultra-thin polarization independent broadband terahertz metamaterial absorber, *Front. Optoelectron.* 14 (2021) 288–297.
- [35] G. S. Yang, F. P. Yan, X. M. Du, T. Li, W. Wang, Y. L. Lv, H. Zhou, Y. F. Hou, Tunable broadband terahertz metamaterial absorber based on vanadium dioxide, *AIP Advances* 12 (2022) 045219.
- [36] S. Asgari, T. Fabritius, Equivalent circuit model of graphene chiral multi-band metadevice absorber composed of U-shaped resonator array, *Optics Express* 28 (2020) 39850–39867.

- [37] C. Liu, L. M. Qi, M. J. Wu, Triple-broadband infrared metamaterial absorber with polarization-independent and wide-angle absorption, *Optics Express* 8 (2018) 2439-2448.
- [38] X. F. Jiao, Z. H. Zhang, T. Li, Y. Xu, G. F. Song, Tunable Dual Broadband Terahertz Metamaterial Absorber Based on Vanadium Dioxide, *Applied Sciences* 10 (2020) 7259.
- [39] J. Huang, J. Li, Y. Yang, J. Li, J. Li, Y. Zhang, J. Yao, Active controllable dual broadband terahertz absorber based on hybrid metamaterials with vanadium dioxide, *Optics Express* 28 (2020) 7018-7027.
- [40] H. L. Feng, Z. X. Zhang, J. Y. Zhang, D. C. Fang, J. C. Wang, C. Liu, T. Wu, G. Wang, L. H. Wang, L. L. Ran, Y. Gao, Tunable Dual-Broadband Terahertz Absorber with Vanadium Dioxide Metamaterial, *Nanomaterials* 12 (2022) 1731.
- [41] K. J. Ri, C. H. Ri, Tunable dual-broadband terahertz metamaterial absorber based on a simple design of slotted VO<sub>2</sub> resonator, *Optics Communications* 536 (2023) 129377.
- [42] K. J. Ri, J. S. Kim, J. H. Kim, C. H. Ri, Tunable triple-broadband terahertz metamaterial absorber using a single VO<sub>2</sub> circular ring, *Optics Communications* 542 (2023) 129573.
- [43] L. Huang, D. R. Chowdhury, S. Ramani, M. T. Reiten, S. N. Luo, A. K. Azad, A. J. Antoinette, J. Talor, H. T. Chen, Impact of resonator geometry and its coupling with ground plane on ultrathin metamaterial perfect absorbers, *Appl. Phys. Lett.* 101 (2012) 101102.
- [44] S. Wang, L. Kang, D. H. Werner, Hybrid Resonators and Highly Tunable Terahertz Metamaterials Enabled by Vanadium Dioxide (VO<sub>2</sub>), *Sci. Rep.* 7 (2017) 4326-4333.
- [45] Y. Zhao, Q. P. Huang, H. L. Cai, X. X. Lin, Y. L. Lua, A broadband and switchable VO<sub>2</sub>-based perfect absorber at the THz frequency, *Optics Communications* 426 (2018) 443-449.
- [46] L. S. Wang, D. Y. Xia, Q. H. Fu, X. Y. Ding, Y. Wang, An electrically switchable wideband metamaterial absorber based on graphene at P band, *Open Physics* 19 (2021) 460-466.
- [47] B. X. Wang, Single-Patterned Metamaterial Structure Enabling Multi-band Perfect Absorption, *Plasmonics* 12 (2017) 95-102.
- [48] X. Y. Peng, B. Wang, S. M. Lai, D. H. Zhang, J. H. Teng, Ultrathin multi-band planar metamaterial absorber based on standing wave resonances, *Optics Express* 20 (2012) 27756-27765.